



This is a repository copy of *Long-range heteronuclear J-coupling constants in esters: Implications for ^{13}C metabolic MRI by side-arm parahydrogen-induced polarization*.

White Rose Research Online URL for this paper:
<http://eprints.whiterose.ac.uk/160339/>

Version: Accepted Version

Article:

Stewart, N.J. orcid.org/0000-0001-8358-394X, Kumeta, H., Tomohiro, M. et al. (3 more authors) (2018) Long-range heteronuclear J-coupling constants in esters: Implications for ^{13}C metabolic MRI by side-arm parahydrogen-induced polarization. *Journal of Magnetic Resonance*, 296. pp. 85-92. ISSN 1090-7807

<https://doi.org/10.1016/j.jmr.2018.08.009>

Article available under the terms of the CC-BY-NC-ND licence
(<https://creativecommons.org/licenses/by-nc-nd/4.0/>).

Reuse

This article is distributed under the terms of the Creative Commons Attribution-NonCommercial-NoDerivs (CC BY-NC-ND) licence. This licence only allows you to download this work and share it with others as long as you credit the authors, but you can't change the article in any way or use it commercially. More information and the full terms of the licence here: <https://creativecommons.org/licenses/>

Takedown

If you consider content in White Rose Research Online to be in breach of UK law, please notify us by emailing eprints@whiterose.ac.uk including the URL of the record and the reason for the withdrawal request.



eprints@whiterose.ac.uk
<https://eprints.whiterose.ac.uk/>

Manuscript Number: JMR-18-157R1

Title: Long-range Heteronuclear J-coupling constants in Esters:
Implications for ^{13}C Metabolic MRI by Side-Arm Parahydrogen-Induced
Polarization

Article Type: Article

Keywords: CLIP-HSQMBC;
DFT simulations;
esters;
hyperpolarized ^{13}C NMR;
long-range heteronuclear J couplings;
sel-HSQMBC-TOCSY;
side-arm parahydrogen induced polarization

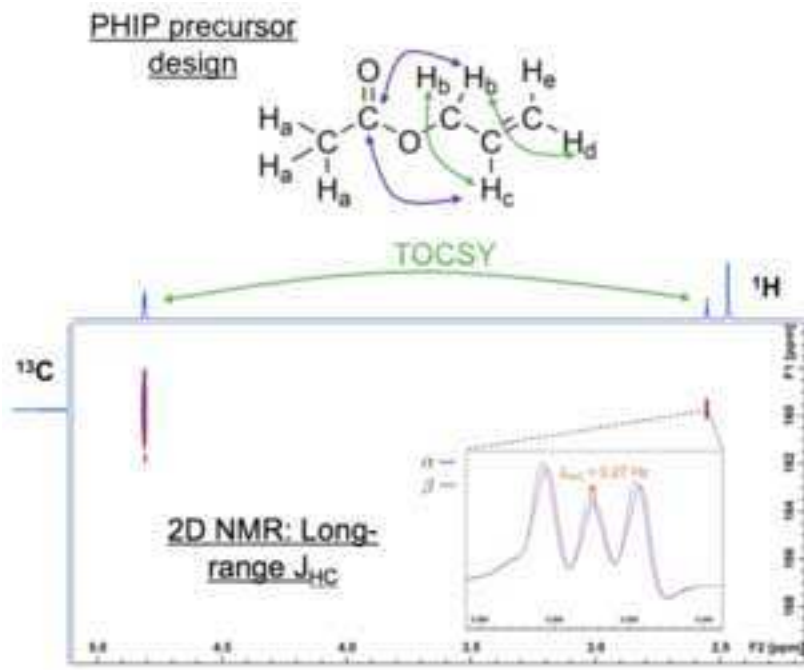
Corresponding Author: Professor Shingo Matsumoto, Ph.D.

Corresponding Author's Institution: Hokkaido University

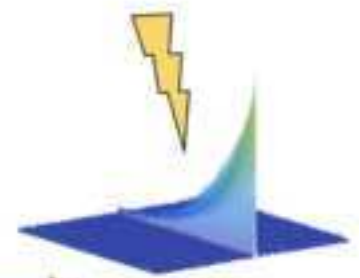
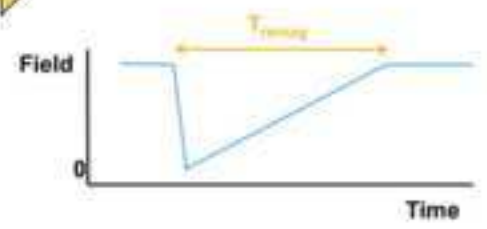
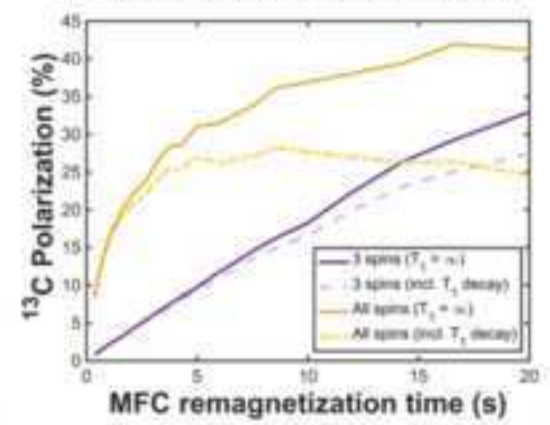
First Author: Neil J Stewart, Ph.D.

Order of Authors: Neil J Stewart, Ph.D.; Hiroyuki Kumeta, Ph.D.; Mitsushi Tomohiro, B.Eng.; Takuya Hashimoto, Ph.D.; Noriyuki Hatae, Ph.D.; Shingo Matsumoto, Ph.D.

Abstract: Side-arm parahydrogen induced polarization (PHIP-SAH) presents a cost-effective method for hyperpolarization of ^{13}C metabolites (e.g. acetate, pyruvate) for metabolic MRI. The timing and efficiency of typical spin order transfer methods including magnetic field cycling and tailored RF pulse sequences crucially depends on the heteronuclear J coupling network between nascent parahydrogen protons and ^{13}C , post-parahydrogenation of the target compound. In this work, heteronuclear nJHC ($1 < n \leq 5$) couplings of acetate and pyruvate esters pertinent for PHIP-SAH were investigated experimentally using selective HSQMBC-based pulse sequences and numerically using DFT simulations. The CLIP-HSQMBC technique was used to quantify 2/3-bond JHC couplings, and 4/5-bond JHC $\lesssim 0.5$ Hz were estimated by the sel-HSQMBC-TOCSY approach. Experimental and numerical (DFT-simulated) nJHC couplings were strongly correlated ($P < 0.001$). Implications for ^{13}C hyperpolarization by magnetic field cycling, and PH-INEPT and ESOTHERIC type spin order transfer methods for PHIP-SAH were assessed, and the influence of direct nascent parahydrogen proton to ^{13}C coupling when compared with indirect TOCSY-type transfer through intermediate (non-nascent parahydrogen) protons was studied by the density matrix approach.



Polarization transfer optimization



Highlights:

- 4-5 bond heteronuclear J_{HC} couplings in esters for PHIP-SAH are extremely small
- Accurate measurement of small J_{HC} requires specialized sequences or DFT simulations
- PHIP polarization transfer in allyl esters may be facilitated by TOCSY-type homonuclear coupling relays
- Optimization of PHIP transfer efficiency must consider the whole coupling network

Long-range Heteronuclear J-coupling constants in Esters: Implications for ^{13}C Metabolic MRI by Side-Arm Parahydrogen-Induced Polarization

*Neil J Stewart*¹, *Hiroyuki Kumeta*^{2,3}, *Mitsushi Tomohiro*¹, *Takuya Hashimoto*^{4,5}, *Noriyuki Hatae*⁶, *Shingo Matsumoto*^{1,7*}

1: Division of Bioengineering and Bioinformatics, Graduate School of Information Science and Technology, Hokkaido University, Sapporo, Japan

2: Department of Structural Biology, Faculty of Advanced Life Science, Hokkaido University, Sapporo, Japan

3: Global Station for Soft Matter, Global Institution for Collaborative Research and Education, Hokkaido University, Sapporo, Japan

4: Department of Chemistry, Graduate School of Science, Kyoto University, Kyoto, Japan

5: Department of Chemistry, Graduate School of Science, Chiba University, Chiba, Japan

6: School of Pharmaceutical Sciences, Health Sciences University of Hokkaido, Ishikari-Tobetsu, Japan

7: JST, PREST, Saitama, Japan

*: Corresponding author, Shingo Matsumoto, Magnetic Resonance Engineering Laboratory, Division of Bioengineering and Bioinformatics, Graduate School of Information Science and Technology, Hokkaido University, North 14, West 9, Kita-ku, Sapporo, Hokkaido 060-0814, Japan. smatsumoto@ist.hokudai.ac.jp

Keywords: CLIP-HSQMBC; DFT simulations; esters; hyperpolarized ^{13}C NMR; long-range heteronuclear J couplings; sel-HSQMBC-TOCSY; side-arm parahydrogen induced polarization

Word count (main text: 3608, no limit)

Graphical abstract & Highlights: see separate files

Abstract:

Side-arm parahydrogen induced polarization (PHIP-SAH) presents a cost-effective method for hyperpolarization of ^{13}C metabolites (e.g. acetate, pyruvate) for metabolic MRI. The timing and efficiency of typical spin order transfer methods including magnetic field cycling and tailored RF pulse sequences crucially depends on the heteronuclear J coupling network between nascent parahydrogen protons and ^{13}C , post-parahydrogenation of the target compound. In this work, heteronuclear $^n\text{J}_{\text{HC}}$ ($1 < n \leq 5$) couplings of acetate and pyruvate esters pertinent for PHIP-SAH were investigated experimentally using selective HSQMBC-based pulse sequences and numerically using DFT simulations. The CLIP-HSQMBC technique was used to quantify 2/3-bond J_{HC} couplings, and 4/5-bond $\text{J}_{\text{HC}} \lesssim 0.5$ Hz were estimated by the sel-HSQMBC-TOCSY approach. Experimental and numerical (DFT-simulated) $^n\text{J}_{\text{HC}}$ couplings were strongly correlated ($P < 0.001$). Implications for ^{13}C hyperpolarization by magnetic field cycling, and PH-INEPT and ESOTHERIC type spin order transfer methods for PHIP-SAH were assessed, and the influence of direct nascent parahydrogen proton to ^{13}C coupling when compared with indirect TOCSY-type transfer through intermediate (non-nascent parahydrogen) protons was studied by the density matrix approach.

Introduction:

Hyperpolarization refers to nuclear polarization many orders of magnitude above Boltzmann polarization, and is associated with dramatic signal enhancement in magnetic resonance (MR), with applications in noble gas MR imaging of the lungs [1] and solution-state ^{13}C MR of pyruvate metabolism [2]. Parahydrogen-induced polarization (PHIP) [3–6] presents a relatively cost-effective alternative to dynamic nuclear polarization (DNP) for hyperpolarization of ^{13}C compounds for solution-state metabolic MR applications. PHIP of ^{13}C requires two steps: (i) PH addition to an unsaturated C-C bond of a target compound, to break the symmetry of the PH molecule and generate ^1H hyperpolarization [3], (ii) polarization transfer from ^1H to a nuclei of interest (usually ^{13}C , ^{15}N) on the same compound. For this PHIP approach, an unsaturated C-C bond is required for hydrogenation, and as such the choice of suitable compounds has been limited to date, restricting *in vivo* applications predominantly to angiography [7]. However, the recent development of side-arm PHIP (PHIP-SAH) [8,9], wherein the unsaturated alcohol (side-arm) of an ester is hydrogenated and polarization is transferred to the carboxylate group ^{13}C , enables the realization of hyperpolarized metabolites such as acetate or pyruvate after side-arm cleavage, and has recently been shown feasible for *in vivo* metabolic MRI applications [10]. We also note that an alternative approach, Signal Amplification by Reversible Exchange (SABRE), permits unsaturated compounds to be polarized by PHIP by using an intermediate metal catalyst for PH-substrate polarization transfer such that the substrate is not chemically modified [11,12], however hyperpolarized ^{13}C -pyruvate has yet to be realized by this technique.

In conventional PHIP, ^1H - ^{13}C polarization transfer is typically induced by RF pulse sequences [13–16] or magnetic field cycling (MFC) [17,18], the latter of which exhibits high efficiency for certain compounds pertinent for PHIP-SAH. However, the sequence timing and polarization transfer efficiency of both methods critically depends on the J coupling network of the compound. Whilst PHIP- and SABRE-based techniques have been utilized previously to measure homonuclear and heteronuclear J_{HC}

coupling constants [19,20], there is limited literature regarding heteronuclear J_{HC} couplings in esters appropriate for PHIP-SAH, and in particular, long-range ${}^3J_{\text{HC}}$, ${}^4J_{\text{HC}}$ or ${}^5J_{\text{HC}}$ values are challenging to measure and not well known.

Conventional 2D heteronuclear multiple-bond correlation (HMBC) NMR sequences can often reveal ${}^{2-3}J_{\text{HC}}$, but anti-phase signal cancellation during long inter-pulse delays leads to poor sensitivity when HMBC is optimized for long-range J_{HC} . Thus, several novel techniques have been developed to allow measurement of long-range J_{HC} for accurate structure determination [21]. For example, J-resolved HMBC enables upscaling of J_{HC} and detection in the F_1 dimension, [22] but also suffers from insensitivity. Heteronuclear single quantum multiple bond correlation (HSQMBC) [23] and variants including CLean In-Phase multiplets (CLIP)-HSQMBC [24], long-range (LR)-HSQMBC [25] and J-up-HSQMBC [26] overcome some limitations of HMBC and permit acquisition of in-phase spectral multiplets for relatively simple calculation of long-range heteronuclear couplings. However, these methods do not allow determination of the sign of J couplings, which typically necessitates acquisition of in-phase anti-phase (IPAP) data [27]. The use of IPAP, selective ${}^1\text{H}$ inversion pulses and the addition of a Total Correlation Spectroscopy (TOCSY) block to the HSQMBC sequence (sel-HSQMBC-TOCSY) [28] has been proposed to facilitate measurement of small J_{HC} values in compounds with sufficient protons for efficient TOCSY transfer.

In the absence of a universally-accepted experimental method for analysis of ${}^nJ_{\text{HC}}$ ($n>1$), numerical methods, typically based on density functional theory (DFT), have also been established [29,30]. However, whilst several reports of ${}^2J_{\text{HC}}$ and ${}^3J_{\text{HC}}$ derived by DFT methods have been published, reports of the evaluation of ${}^nJ_{\text{HC}}$ ($n>3$) are scarce [31].

In this work, the ${}^nJ_{\text{HC}}$ ($1<n\leq 5$) couplings of several esters appropriate for PHIP-SAH were characterized experimentally using CLIP-HSQMBC and sel-HSQMBC-TOCSY techniques, and numerically using DFT simulations. The potential impact of our results on achievable ${}^{13}\text{C}$ hyperpolarization by PHIP was studied by the density matrix approach.

Experimental:

Chemicals

^{13}C propargyl pyruvate was synthesized by refluxing [1- ^{13}C]pyruvic acid and propargyl alcohol for 3h in benzene and a catalytic amount of *p*-TsOH \cdot H₂O (as in ref [32]).

[1- ^{13}C]-vinyl acetate was prepared according to a procedure described in the literature [33] (full details in Supporting Information). ^{13}C -labeled ethyl acetate was produced by hydrogenation of ^{13}C vinyl acetate using a palladium catalyst. [1- ^{13}C]allyl acetate was prepared using sodium acetate as described in the Supporting Information. Ethyl propionate was purchased with ^{13}C in natural abundance (TCI, Tokyo, Japan). The structures of all compounds studied are depicted in Figure 1.

NMR measurements

All esters were dissolved in CDCl₃. Conventional ^1H spectroscopy and proton-coupled ^{13}C spectroscopy data were acquired on a JEOL ECS400C (Delta V5.0.4) 400 MHz spectrometer. Coupled ^{13}C spectroscopy parameters: decoupling off; number of points 65536 or 131072; flip angle 30°; sweep width 200 ppm. All 2D NMR, including conventional HMBC data, were acquired on a Bruker Avance III HD (TopSpin 3.1) 800 MHz spectrometer equipped with a 5 mm z-gradient PATXI probe. HMBC parameters: spectral width 13.0 and 210 ppm in F2 and F1, respectively; number of points 2048 and 256, number of scans 16. Individual CLIP-HSQMBC acquisitions [24] were carried out for each hydrogen group of interest, with the following parameters: 20 ms Gaussian selective refocusing pulse for ^1H , spectral width 4.0 and 180 ppm in F2 and F1, respectively; number of points 8192 (or 16384) and 128, number of scans 16 or 32. For extraction of the sign and magnitude of small couplings, sel-HSQMBC-TOCSY [28] was employed with the following parameters: 20 ms Gaussian selective refocusing pulse for ^1H , spectral width 8.0 and 180 ppm in F2 and F1, respectively; number of points 8192 (or 16384) and 128, number of scans 32 or 64. All other RF pulse, phase cycling and acquisition parameters were set as per the original references [24,28]. IP and AP data were acquired sequentially, FIDs were added/subtracted and J_{HC} values were extracted from the corresponding shift in $\alpha = \text{IP} + \text{AP}$ and $\beta = \text{IP} - \text{AP}$ data for the

^{13}C projection of interest. 3-bond couplings were taken as a reference to determine the sign of 4- and 5-bond couplings. Sign assignment was verified by DFT simulations as described below.

Multiplet analysis of 1D NMR spectroscopy data was carried out in MestReNova V12.0.2 (Metrelab Research S.L.) or Bruker Topspin 4.0 after zero-filling by a factor of 2 and exponential and trapezoidal apodization. 2D NMR data analysis was performed in TopSpin 3.1 or 4.0, after zero-filling by a factor of 2 in F2 and 4 in F1, and applying a two-dimensional sine bell apodization function.

DFT Simulations

For each compound, a molecular conformational search was performed using Spartan (Wavefunction Inc. Irvine, CA) with 10000 candidate conformers and the Merck Molecular Force Field (MMFF) model. For each resultant conformer, DFT simulations were carried out using Gaussian 16 [34]. After geometry optimization of each conformer using the B3LYP functional and 6-311++G(d,p) basis set, all homonuclear and heteronuclear J coupling constants were calculated using the conventional GIAO orbitals, B3LYP functional and both 6-311++G(d,p) and EPR-III basis sets in combination with the Gaussian “mixed” keyword (which employs an augmented basis set for Fermi contact terms). Python scripts as described in refs [35,36] were modified in order to check each conformer for imaginary frequencies, generate batch scripts for Gaussian commands, and to perform resultant Boltzmann-weighted averaging of coupling constants.

Density Matrix Simulations

Simulations of magnetic field cycling, PH-INEPT+ and ESOTHERIC polarization transfer schemes for PHIP were carried out in Matlab (Mathworks, Natick, MA) using a density matrix approach similar to that in refs [15,18], in order to assess the effect of the various components of the J coupling network on the polarization transfer efficiency. Firstly, a simple 3-spin (nascent para- $\text{H}_2 + ^{13}\text{C}$) network was considered and J_{HC} , J_{H1C} values were varied between at a fixed $J_{\text{HH1}} = 7.5$ Hz [37] to evaluate the sensitivity of

each method to J coupling magnitude and difference $\Delta J_{\text{HC}} = J_{\text{HC}} - J_{\text{H1C}}$. Subsequently, for allyl acetate, in which the direct couplings between nascent parahydrogen protons and ^{13}C occur over 4 or 5 bonds, the effect of TOCSY-type transfer to neighboring (non-nascent parahydrogen) protons and potential relay to ^{13}C was considered by including all relevant spins and associated derived couplings, and achievable polarization by magnetic field cycling was quantified. Additional details of the density matrix approach can be found in the Supporting Information.

Results:

Heteronuclear J_{HC} values simulated using the DFT basis sets 6-311++G(d,p) and EPR-III agreed to a high level of accuracy (Spearman's rho 0.999, $P < 0.001$). The absolute difference between the values derived from these basis sets tended to increase as the absolute value of J_{HC} increased (see Bland-Altman analysis in Supporting Information, Figure S1). Experimentally derived J_{HC} values, combined from ^{13}C spectroscopy, CLIP-HSQMBC and sel-HSQMBC-TOCSY data, are summarized in Table 1 and plotted against DFT-derived values (6-311++G(d,p) basis set) in Figure 2. Experimental and DFT J_{HC} values were strongly correlated ($r=0.965$, $P<0.001$, Figure 2a) and exhibited a mean absolute difference of 0.22 Hz (indicating a slight bias to higher experimentally-derived J_{HC} , Figure 2b).

CLIP-HSQMBC was able to distinguish couplings that could not be resolved from ^{13}C spectroscopy multiplet analysis, and was found to be particularly suitable for $^2J_{\text{HC}}$ and $^3J_{\text{HC}}$ measurements. Conventional HMBC and CLIP-HSQMBC typically showed crosspeaks for couplings ≥ 0.5 Hz, but did not exhibit crosspeaks corresponding to the $^{4-5}J_{\text{HC}}$ in EA, EPR or AA. Figure 3 illustrates representative HMBC data from vinyl and ethyl acetate; two low-intensity crosspeaks from J_{HcCl} and J_{HdCl} could be observed in VA, whilst the 4-bond J_{HcCl} coupling in EA did not yield a crosspeak, suggesting the coupling is ≤ 0.5 Hz.

In cases where CLIP-HSQMBC data did not exhibit a crosspeak or the peak could not easily be resolved (typically those $< 1\text{Hz}$), sel-HSQMBC-TOCSY was required to estimate coupling values. Figures 4 and 5 illustrate the estimation of the $^3J_{\text{HaCl}}$ and $^5J_{\text{HcCl}}$ couplings in propargyl pyruvate, by CLIP-HSQMBC and

sel-HSQMBC-TOCSY, respectively. In Figure 4, the Ha protons were selectively excited to eliminate all other coupling pathways, and in Figure 5, the Hb protons were excited to investigate the relayed transfer between Hb-¹³C and Hb-Hc.

Density matrix simulations of achievable ¹³C polarization by spin order transfer with magnetic field cycling and RF pulse sequence approaches in a simple three-spin (para-H₂, ¹³C1) system are depicted in Figure 6. J_{HH1} was assumed to equal 7.5 Hz and the absolute value and difference of the two heteronuclear J_{HC} values was varied. In a), the remagnetization time from zero field to 1500 nT was fixed at 5 sec. In b) and c), the PH-INEPT+ and ESOTHERIC inter-pulse timings were varied to determine the optimum polarization for each J coupling condition. These contour plots indicate that when considering direct heteronuclear polarization transfer from nascent PH protons to ¹³C, a significant difference in J_{HC} between the two PH atoms is required, and at least one J_{HC} should be sufficiently larger than 0. Considering parahydrogenation of vinyl acetate, the ³⁻⁴J_{HC} quoted in Table 1 for ethyl acetate suggest an approximate achievable polarization of >80%, by MFC and ESOTHERIC, or ~45% by PH-INEPT+ (ignoring relaxation and assuming a 3-spin system).

In allyl acetate, the ⁴⁻⁵J_{HC} were found to be extremely small and optimized magnetic field cycling in the three-spin (para-H₂, ¹³C1) system was predicted to yield a relatively low ¹³C polarization (~10% at remagnetization time of 5 sec, ignoring relaxation, see Figure 7). However, considering the entire J coupling network in allyl acetate (including simulated homonuclear J_{HH} couplings, and all experimentally-measured heteronuclear J_{HC} couplings), density matrix simulation of MFC polarization transfer efficiency revealed that for remagnetization times < 20 s, improved ¹³C polarization may be obtained (e.g. ~31% at remagnetization time of 5 sec, ignoring relaxation, Figure 7).

Discussion:

Application of the latest developments in 2D NMR pulse sequences sensitized to long-range heteronuclear J_{HC} couplings, along with DFT simulations, has enabled the evaluation of the full heteronuclear J_{HC} coupling network in esters that are suitable

precursors for PHIP-SAH metabolic MR applications. Our results have implications for the optimization of the timings and achievable polarization of ^{13}C for magnetic field cycling and PH-INEPT+ type polarization transfer sequences.

As mentioned in the Results, Figure 6 suggests that ethyl acetate may be efficiently polarized by PH-INEPT+ and ESOTHERIC based methods, to achieve ^{13}C polarization $> 40\%$ and $> 80\%$, respectively. Similarly, field cycling exhibits theoretical values of ^{13}C polarization $> 80\%$ when ignoring relaxation and considering only a 3-spin system. However, inclusion of all neighboring heteronuclear and homonuclear couplings with non-nascent-parahydrogen “spectator” protons leads to significant polarization losses (max polarization $\sim 25\text{-}30\%$) for the field cycling approach (see Supporting Information Figure S2). Others have reported similar polarization reductions when considering couplings to and between spectator protons in other compounds [18,38]. At present, there is a lack of effective methods for high-yield production of vinyl pyruvate, which limits possible PHIP ^{13}C MR applications to acetate (after hydrogenation of vinyl acetate and side-arm cleavage). In vivo studies of acetate metabolism show some promise [39] and may offer complementary information to pyruvate metabolism studies. We note that during preparation of the present paper, a report was published which shows the experimental application of the ESOTHERIC method to obtain a polarization of $\sim 60\%$ on ethyl acetate [40].

In this work, although propargyl pyruvate was studied, allyl acetate (rather than allyl pyruvate) was chosen for investigation as it was easily available to our laboratory. If one was to hydrogenate propargyl pyruvate in the same manner as was done for our vinyl acetate sample (to ethyl acetate), reduction would proceed rapidly to yield the single-bonded propyl pyruvate. On the other hand, controlled hydrogenation would yield allyl pyruvate, but in relatively low concentration, limiting NMR sensitivity. Thus, it is pertinent to assume that the J coupling network relevant for PHIP-SAH is not significantly different between allyl acetate and allyl pyruvate.

The accuracy of $^{2-3}J_{\text{HC}}$ derived from DFT simulations is assumed to be $\leq \pm 0.5$ Hz (Gaussian support, *personal communication*). However, simulated values for 4/5 bond couplings were typically extremely low and potentially less reliable than experimental measurements (Figure 2). We note that there are alternatives to conventional DFT approaches, such as the relativistic force field (RFF) approach that uses a reduced basis

set for accelerated calculations [41]. The RFF approach has been employed for estimation of both J_{HH} and J_{HC} , however to date it has not been applied to ${}^nJ_{HC}$ for $n > 3$ [42], and unfortunately depends on empirical parameters [30]. At present, we may propose that for PHIP-SAH, 4/5 bond couplings require estimation with the sel-HSQMBC-TOCSY experiment, whilst 2/3 bond couplings can be predicted by DFT simulation to a reasonable level of accuracy, and validated with CLIP-HSQMBC if required.

Quantification of the accuracy of sel-HSQMBC-TOCSY is challenging due to the lack of relevant literature. However, we note that in their original paper, Sauri et al reported couplings as low as -0.4 Hz [28], and in subsequent work, values ~ 0.2 Hz were reported [43]. We thus postulate that the uncertainty of these very long-range couplings is around ± 0.1 Hz, although we acknowledge that the uncertainty could be higher depending on the experimental spectral resolution used and complexity of the 1H splitting pattern.

There is relatively little literature dealing with the 4 and 5 bond J_{HC} in these esters. However, we note that the experimentally derived ${}^4J_{HC}$ values for ethyl propionate (Table 1) are in strong disagreement with a previous report of 1.7 Hz [18]. The methods for J_{HC} coupling calculation are not reported in that paper, but it is worth noting that 1.7 Hz is larger than 4-bond J_{HC} values reported in other compounds (typically < 1.0 Hz) [25,31], although the differing chemistry must be considered. Our result of an extremely low ${}^4J_{HC}$ is supported by the absence of a corresponding peak in the HMBC and CLIP-HSQMBC spectra, and a high ratio of IP/AP crosspeak signal in sel-HSQMBC-TOCSY data; this ratio asymptotes to infinity upon J_{HC} tending to 0 Hz (see supporting information of [25]). For similar reasons, we believe the 4 and 5 J_{HC} estimates for allyl pyruvate (~ 1.0 Hz) reported in supporting information of [9] may require further verification, referring to Figures 6 and 7 of the present manuscript.

Figures 6 and 7 indicate that considering direct 4/5-bond transfer for a 3-spin system with such low 4- and 5-bond J_{HC} values as in allyl acetate is likely to yield low polarization on ${}^{13}C$, particularly at remagnetization times < 20 s. However, our experimental and numerical measurements of heteronuclear couplings – used in combination with simulated homonuclear J_{HH} couplings – suggest that experimental conditions similar to those used by Cavallari et al [9] could lead to a ${}^{13}C$ polarization \sim

27% in allyl acetate; when including all neighboring spin-spin coupling constants and approximate relaxation effects as discussed below (see Figure 7; at a remagnetization time of 5 sec). Thus it appears that a strong homonuclear coupling network, in addition to heteronuclear 3-bond polarization transfer, is critical for efficient polarization transfer. In other words, the relatively strong $^3J_{\text{HbCl}}$ (3.15 Hz) is fed with polarization by the strong homonuclear couplings (5.9 Hz $^2J_{\text{HbHc}}$ and 11.4 Hz $^3J_{\text{HcHd}}$) involving the two nascent parahydrogen protons. We therefore postulate that TOCSY-type interactions with spectator spins are crucial to improve the efficiency of polarization transfer from nascent parahydrogen protons to ^{13}C in allyl acetate (or by inference, pyruvate), but that the opposite is true for ethyl acetate (pyruvate) (i.e. interactions with spectator spins lead to polarization losses).

Taking the T_1 relaxation times at Earth's field to be ~ 29 sec for nascent parahydrogen protons (measured by the ALTADENA "waiting" method at Earth's field [44] and recording the NMR signal on a 1.5 T system) and the carboxylate ^{13}C $T_1 = 89$ s (reported for allyl pyruvate at Earth's field [9]), and multiplying the allyl acetate MFC polarization transfer time evolution by the corresponding exponentials, the resulting allyl acetate MFC profile exhibits a maximum obtainable ^{13}C polarization at ~ 5 -10 sec (see Figure 7), which is of the same order as the experimental empirical optimum condition of 4 sec reported by Cavallari et al [9]. We note that the individual magnetic field cycling spin order build-up curves for ^{13}C showed secondary peaks at $t < 20$ sec for very slow remagnetization rates. Thus, for remagnetization rates that would normally require remagnetization time > 20 sec, we can consider halting spin order transfer at that secondary peak and rapidly (adiabatically) increasing the field to zero field in order to maintain reasonable polarization levels. This was found to result in a fairly constant polarization for $t > 20$ sec (when relaxation effects were included). It is worth noting that multiplying the polarization transfer time evolution by exponentials is only an approximation of the true relaxation during field cycling. Full description of relaxation during periods of spin state evolution requires accounting for cross relaxation in the coupled spin system, and knowledge of the correlation time [45] (see [46] for an example in $^{15}\text{NH}_4^+$), and in practice relaxation is seldom considered in density matrix simulations. In addition, the estimated relaxation times quoted above are strongly dependent on magnetic field, and furthermore we assume that relaxation behavior for allyl acetate and pyruvate is the same, thus caution must be taken when adopting the

above values. Ideally, comprehensive studies of the field dependence of ^{13}C T_1 (as per Chattergoon et al. [47]) should be performed for each compound of interest.

Although PH-INEPT+ and similar methods typically assume a 3-spin system with direct coupling, in future work it may be feasible to develop a novel pulse sequence and accompanying density matrix simulations to permit polarization transfer by RF pulses with inter-pulse timings dependent on the homonuclear TOCSY-type transfer in addition to the 3-bond heteronuclear coupling. Alternatively, if a double- or fully-labeled ^{13}C sample could be synthesized, an additional evolution period could be added to the ESOTHERIC RF pulse sequence to exploit ^{13}C - ^{13}C coupling for polarization transfer, during ^1H decoupling (as in the ESOTHERIC variant discussed in [16]). This could potentially yield improved polarization transfer efficiency in allyl acetate, in a similar manner to that demonstrated by the proposed model of ^1H - ^1H TOCSY-type homonuclear transfer and 3-bond heteronuclear transfer discussed above.

Finally, we draw further notice to the recent realization of ^{13}C pyruvate and acetate by PHIP-SAH of cinnamyl esters using the ESOTHERIC method [16]. Cinnamyl esters offer a readily-cleavable side-arm and feasible separation of organic and aqueous phases to provide a clean solution for injection for *in vivo* ^{13}C metabolic NMR applications, as an alternative to allyl acetate/pyruvate. Although optimum polarization transfer for pyruvate precursors requires a relatively expensive deuterated, double- ^{13}C -labeled sample, it may be envisaged possible to use a single-labeled, non-deuterated cinnamyl ester sample in combination with MFC by exploiting TOCSY-type ^1H - ^1H spin order transfer to induce sufficient ^{13}C polarization for *in vivo* MR in the future.

Conclusion:

The heteronuclear J_{HC} coupling network in several esters pertinent to PHIP-SAH for metabolic MRI has been investigated by employing long-range J_{HC} sensitized CLIP-HSQMBC and sel-HSQMBC-TOCSY experiments, and DFT simulations. Our measurements suggest that high experimental polarization transfer should be realizable in allyl esters for production of hyperpolarized ^{13}C acetate and pyruvate for high quality *in vivo* metabolic MR in the near future. Additionally, our results should facilitate

improved characterization of polarization transfer efficiency by MFC and RF pulse sequence (PH-INEPT and ESOTHERIC) methods via accurate simulations and calculation of precise timings by considering both heteronuclear and homonuclear TOCSY-type relayed polarization transfer.

Acknowledgements: Yoshiki Uchio and Yuka Fukue (Hokkaido University) for technical assistance. Fernando Clemente (Gaussian Inc.), Martin Dračinský (Czech Academy of Sciences), Trygve Helgaker (University of Oslo) for technical support with DFT simulations. Teodor Parella (Universitat Autònoma de Barcelona), Klaus Zangger (University of Graz) for pulse sequence support. NJS is an international research fellow of the Japanese Society for the Promotion of Science (JSPS).

References:

- [1] S.B. Fain, F.R. Korosec, J.H. Holmes, R. O'Halloran, R.L. Sorkness, T.M. Grist, Functional lung imaging using hyperpolarized gas MRI, *J. Magn. Reson. Imaging*. 25 (2007) 910–923. doi:10.1002/jmri.20876.
- [2] S.J. Nelson, J. Kurhanewicz, D.B. Vigneron, P.E.Z. Larson, A.L. Harzstark, M. Ferrone, M. van Criekinge, J.W. Chang, R. Bok, I. Park, G. Reed, L. Carvajal, E.J. Small, P. Munster, V.K. Weinberg, J.H. Ardenkjaer-Larsen, A.P. Chen, R.E. Hurd, L.-I. Odegardstuen, F.J. Robb, J. Tropp, J.A. Murray, Metabolic Imaging of Patients with Prostate Cancer Using Hyperpolarized [1-13C]Pyruvate, *Sci. Transl. Med.* 5 (2013) 198ra108-198ra108. doi:10.1126/scitranslmed.3006070.
- [3] C.R. Bowers, D.P. Weitekamp, Parahydrogen and Synthesis Allow Dramatically Enhanced Nuclear Alignment, *J. Am. Chem. Soc.* 109 (1987) 5541–5542. doi:10.1021/ja00252a049.
- [4] R. Eisenberg, Parahydrogen-Induced Polarization: A New Spin on Reactions with H₂, *Acc. Chem. Res.* 24 (1991) 110–116. doi:10.1021/ar00004a004.
- [5] J. Natterer, J. Bargon, Parahydrogen induced polarization, *Prog. Nucl. Magn. Reson. Spectrosc.* 31 (1997) 293–315. doi:10.1016/S0079-6565(97)00007-1.
- [6] S.B. Duckett, R.E. Mewis, Application of para hydrogen induced polarization techniques in NMR spectroscopy and imaging, *Acc. Chem. Res.* 45 (2012) 1247–1257. doi:10.1021/ar2003094.

- [7] K. Golman, O. Axelsson, H. Jóhannesson, S. Månsson, C. Olofsson, J.S. Petersson, Parahydrogen-induced polarization in imaging: Subsecond ^{13}C angiography, *Magn. Reson. Med.* 46 (2001) 1–5. doi:10.1002/mrm.1152.
- [8] F. Reineri, T. Boi, S. Aime, ParaHydrogen Induced Polarization of ^{13}C carboxylate resonance in acetate and pyruvate, *Nat. Commun.* 6 (2015) 5858. doi:10.1038/ncomms6858.
- [9] E. Cavallari, C. Carrera, S. Aime, F. Reineri, Studies to enhance the hyperpolarization level in PHIP-SAH-produced ^{13}C -pyruvate, *J. Magn. Reson.* 289 (2018) 12–17. doi:10.1016/j.jmr.2018.01.019.
- [10] E. Cavallari, C. Carrera, M. Sorge, G. Bonne, A. Muchir, S. Aime, F. Reineri, The ^{13}C hyperpolarized pyruvate generated by ParaHydrogen detects the response of the heart to altered metabolism in real time, *Sci. Rep.* 8 (2018) 8366. doi:10.1038/s41598-018-26583-2.
- [11] S.S. Roy, K.M. Appleby, E.J. Fear, S.B. Duckett, SABRE-Relay: A Versatile Route to Hyperpolarization, *J. Phys. Chem. Lett.* 9 (2018) 1112–1117. doi:10.1021/acs.jpcclett.7b03026.
- [12] J.B. Hövener, N. Schwaderlapp, R. Borowiak, T. Lickert, S.B. Duckett, R.E. Mewis, R.W. Adams, M.J. Burns, L.A.R. Highton, G.G.R. Green, A. Olaru, J. Hennig, D. Von Elverfeldt, Toward biocompatible nuclear hyperpolarization using signal amplification by reversible exchange: Quantitative in situ spectroscopy and high-field imaging, *Anal. Chem.* 86 (2014) 1767–1774. doi:10.1021/ac403653q.
- [13] S.B. Duckett, C.L. Newell, R. Eisenberg, More than INEPT: Parahydrogen and INEPT+ Give Unprecedented Resonance Enhancement to ^{13}C by Direct ^1H Polarization Transfer, *J. Am. Chem. Soc.* 115 (1993) 1156–1157. doi:10.1021/ja00056a054.
- [14] M. Haake, J. Natterer, J. Bargon, Efficient NMR pulse sequences to transfer the parahydrogen-induced polarization to hetero nuclei, *J. Am. Chem. Soc.* 118 (1996) 8688–8691. doi:10.1021/ja960067f.
- [15] S. Bär, T. Lange, D. Leibfritz, J. Hennig, D. Von Elverfeldt, J.B. Hövener, On the spin order transfer from parahydrogen to another nucleus, *J. Magn. Reson.* 225 (2012) 25–35. doi:10.1016/j.jmr.2012.08.016.
- [16] S. Korchak, S. Yang, S. Mamone, S. Glögler, Pulsed Magnetic Resonance to Signal-Enhance Metabolites within Seconds by utilizing para-Hydrogen,

- ChemistryOpen. 7 (2018) 344–348. doi:10.1002/open.201800024.
- [17] H. Jóhannesson, O. Axelsson, M. Karlsson, Transfer of para-hydrogen spin order into polarization by diabatic field cycling, *Comptes Rendus Phys.* 5 (2004) 315–324. doi:10.1016/j.crhy.2004.02.001.
- [18] E. Cavallari, C. Carrera, T. Boi, S. Aime, F. Reineri, Effects of Magnetic Field Cycle on the Polarization Transfer from Parahydrogen to Heteronuclei through Long-Range J-Couplings, *J. Phys. Chem. B.* 119 (2015) 10035–10041. doi:10.1021/acs.jpcc.5b06222.
- [19] B. A Messerle, C. J Sleigh, M. G Partridge, S. B Duckett, Structure and dynamics in metal phosphine complexes using advanced NMR studies with para-hydrogen induced polarisation, *J. Chem. Soc. Dalt. Trans.* 0 (1999) 1429. doi:10.1039/a809948k.
- [20] N. Eshuis, R.L.E.G. Aspers, B.J.A. Van Weerdenburg, M.C. Feiters, F.P.J.T. Rutjes, S.S. Wijmenga, M. Tessari, Determination of long-range scalar ^1H - ^1H coupling constants responsible for polarization transfer in SABRE, *J. Magn. Reson.* 265 (2016) 59–66. doi:10.1016/j.jmr.2016.01.012.
- [21] T. Parella, J.F. Espinosa, Long-range proton-carbon coupling constants: NMR methods and applications, *Prog. Nucl. Magn. Reson. Spectrosc.* 73 (2013) 17–55. doi:10.1016/j.pnmrs.2013.07.001.
- [22] K. Furihata, H. Seto, J-Resolved HMBC, a new NMR technique for measuring heteronuclear long-range coupling constants, *Tetrahedron Lett.* 40 (1999) 6271–6275. doi:10.1016/S0040-4039(99)01233-2.
- [23] R.T. Williamson, B.L. Márquez, W.H. Gerwick, K.E. Kövér, One- and two-dimensional gradient-selected HSQMBC NMR experiments for the efficient analysis of long-range heteronuclear coupling constants, *Magn. Reson. Chem.* 38 (2000) 265–273. doi:10.1002/(SICI)1097-458X(200004)38:4<265::AID-MRC637>3.0.CO;2-#.
- [24] J. Saurí, T. Parella, J.F. Espinosa, CLIP-HSQMBC: easy measurement of small proton-carbon coupling constants in organic molecules, *Org. Biomol. Chem.* 11 (2013) 4473. doi:10.1039/c3ob40675j.
- [25] R.T. Williamson, A. V. Buevich, G.E. Martin, T. Parella, LR-HSQMBC: A sensitive NMR technique to probe very long-range heteronuclear coupling pathways, *J. Org. Chem.* 79 (2014) 3887–3894. doi:10.1021/jo500333u.

- [26] S. Glanzer, O. Kunert, K. Zangger, Determination of unresolved heteronuclear scalar coupling constants by J(up)-HSQMBC, *J. Magn. Reson.* 268 (2016) 88–94. doi:10.1016/j.jmr.2016.05.002.
- [27] S. Gil, J.F. Espinosa, T. Parella, IPAP-HSQMBC: Measurement of long-range heteronuclear coupling constants from spin-state selective multiplets, *J. Magn. Reson.* 207 (2010) 312–321. doi:10.1016/j.jmr.2010.09.017.
- [28] J. Saurí, J.F. Espinosa, T. Parella, A definitive NMR solution for a simple and accurate measurement of the magnitude and the sign of small heteronuclear coupling constants on protonated and non-protonated carbon atoms, *Angew. Chemie - Int. Ed.* 51 (2012) 3919–3922. doi:10.1002/anie.201108959.
- [29] A. Bagno, F. Rastrelli, G. Saielli, Toward the complete prediction of the ¹H and ¹³C NMR spectra of complex organic molecules by DFT methods: Application to natural substances, *Chem. - A Eur. J.* 12 (2006) 5514–5525. doi:10.1002/chem.200501583.
- [30] T. Helgaker, M. Jaszuński, P. Świder, Calculation of NMR Spin-Spin Coupling Constants in Strychnine, *J. Org. Chem.* 81 (2016) 11496–11500. doi:10.1021/acs.joc.6b02157.
- [31] E. Procházková, L. Čechová, P. Jansa, M. Dračinský, Long-range heteronuclear coupling constants in 2,6-disubstituted purine derivatives, *Magn. Reson. Chem.* 50 (2012) 295–298. doi:10.1002/mrc.3806.
- [32] F. Heaney, J. Fenlon, C. O'Mahony, P. McArdle, D. Cunningham, α -Oximono-esters as precursors to heterocycles – generation of oxazinone N-oxides and cycloaddition to alkene dipolarophiles, *Org. Biomol. Chem.* 1 (2003) 4302–4316. doi:10.1039/B307077H.
- [33] R. V. Shchepin, D.A. Barskiy, A.M. Coffey, I. V. Manzanera Esteve, E.Y. Chekmenev, Efficient Synthesis of Molecular Precursors for Para-Hydrogen-Induced Polarization of Ethyl Acetate-¹-¹³C and beyond, *Angew. Chemie - Int. Ed.* 55 (2016) 6071–6074. doi:10.1002/anie.201600521.
- [34] M.J. Frisch, G.W. Trucks, H.B. Schlegel, G.E. Scuseria, M.A. Robb, J.R. Cheeseman, G. Scalmani, V. Barone, G.A. Petersson, H. Nakatsuji, X. Li, M. Caricato, A. V. Marenich, J. Bloino, B.G. Janesko, R. Gomperts, B. Mennucci, H.P. Hratchian, J. V. Ortiz, A.F. Izmaylov, J.L. Sonnenberg, D. Williams-Young, F. Ding, F. Lipparini, F. Egidi, J. Goings, B. Peng, A. Petrone, T. Henderson, D.

- Ranasinghe, V.G. Zakrzewski, J. Gao, N. Rega, G. Zheng, W. Liang, M. Hada, M. Ehara, K. Toyota, R. Fukuda, J. Hasegawa, M. Ishida, T. Nakajima, Y. Honda, O. Kitao, H. Nakai, T. Vreven, K. Throssell, J. Montgomery, J. A., J.E. Peralta, F. Ogliaro, M.J. Bearpark, J.J. Heyd, E.N. Brothers, K.N. Kudin, V.N. Staroverov, T.A. Keith, R. Kobayashi, J. Normand, K. Raghavachari, A.P. Rendell, J.C. Burant, S.S. Iyengar, J. Tomasi, M. Cossi, J.M. Millam, M. Klene, C. Adamo, R. Cammi, J.W. Ochterski, R.L. Martin, K. Morokuma, O. Farkas, J.B. Foresman, D.J. Fox, Gaussian 16, Revision A.03, Gaussian, Inc., Wallingford CT. (2016).
- [35] P.H. Willoughby, M.J. Jansma, T.R. Hoyer, A guide to small-molecule structure assignment through computation of (¹H and ¹³C) NMR chemical shifts, *Nat. Protoc.* 9 (2014) 643–660. doi:10.1038/nprot.2014.042.
- [36] S. Reisbick, P. Willoughby, Generation of Gaussian 09 Input Files for the Computation of ¹H and ¹³C NMR Chemical Shifts of Structures from a Spartan'14 Conformational Search, *Protoc. Exch.* (2014) 1–10. doi:10.1038/protex.2014.015.
- [37] E. Cavallari, C. Carrera, F. Reineri, ParaHydrogen Hyperpolarized Substrates for Molecular Imaging Studies, *Isr. J. Chem.* 57 (2017) 833–84. doi:10.1002/ijch.201700030.
- [38] V.A. Norton, Efficient generation of hyperpolarized molecules utilizing the scalar order of parahydrogen, Diss. (Ph.D.), Calif. Inst. Technol. (2010).
- [39] U. Koellisch, C. Laustsen, T.S. Nørtinger, J.A. Østergaard, A. Flyvbjerg, C. V. Gringeri, M.I. Menzel, R.F. Schulte, A. Haase, H. Stødkilde-Jørgensen, Investigation of metabolic changes in STZ-induced diabetic rats with hyperpolarized [¹⁻¹³C]acetate., *Physiol. Rep.* 3 (2015) e12474. doi:10.14814/phy2.12474.
- [40] S. Korchak, S. Mamone, S. Glöggler, Over 50 % ¹H and ¹³C Polarization for Generating Hyperpolarized Metabolites-A para -Hydrogen Approach, *ChemistryOpen.* (2018). doi:10.1002/open.201800086.
- [41] A.G. Kutateladze, O.A. Mukhina, Relativistic Force Field: Parametrization of ¹³C-¹H Nuclear Spin-Spin Coupling Constants, *J. Org. Chem.* 80 (2015) 10838–10848. doi:10.1021/acs.joc.5b02001.
- [42] G.K. Pierens, T.K. Venkatachalam, D.C. Reutens, Investigation of two- and three-bond carbon–hydrogen coupling constants in cinnamic acid based

- compounds, *Magn. Reson. Chem.* 54 (2016) 941–946. doi:10.1002/mrc.4469.
- [43] J. Saurí, Y. Liu, T. Parella, R.T. Williamson, G.E. Martin, Selecting the Most Appropriate NMR Experiment to Access Weak and/or Very Long-Range Heteronuclear Correlations, *J. Nat. Prod.* 79 (2016) 1400–1406. doi:10.1021/acs.jnatprod.6b00139.
- [44] T. Jonischkeit, U. Bommerich, J. Stadler, K. Woelk, H.G. Niessen, J. Bargon, Generating long-lasting ^1H and ^{13}C hyperpolarization in small molecules with parahydrogen-induced polarization, *J. Chem. Phys.* 124 (2006) 1–5. doi:10.1063/1.2209235.
- [45] L.G. Werbelow, D.M. Grant, Intramolecular Dipolar Relaxation in Multispin Systems, *Adv. Magn. Opt. Reson.* 9 (1977) 189–299. doi:10.1016/B978-0-12-025509-2.50008-7.
- [46] N.D. Werbeck, D.F. Hansen, Heteronuclear transverse and longitudinal relaxation in AX_4 spin systems: Application to ^{15}N relaxations in $^{15}\text{NH}_4^+$, *J. Magn. Reson.* 246 (2014) 136–148. doi:10.1016/j.jmr.2014.06.010.
- [47] N. Chattergoon, F. Martínez-Santesteban, W.B. Handler, J.H. Ardenkjær-Larsen, T.J. Scholl, Field dependence of T_1 for hyperpolarized $[1-^{13}\text{C}]$ pyruvate, *Contrast Media Mol. Imaging.* 8 (2013) 57–62. doi:10.1002/cmml.1494.

Tables:

See separate file

Figure captions:

Figure 1: Illustration of the esters investigated in this study. VA: vinyl acetate, EA: ethyl acetate, PP: propargyl pyruvate, AA: allyl acetate, EPR: ethyl propionate. ^{13}C -labeled samples are indicated by the green ^{13}C at the C1 position. In all cases, the carboxyl carbon represents the carbon of interest for generating hyperpolarized metabolites (e.g. pyruvate) and is typically ^{13}C -labeled in a hyperpolarization experiment. Ethyl and allyl esters are the products of hydrogenation of vinyl or propargyl esters, respectively and

thus suitable PHIP targets. The *nascent* parahydrogen protons would correspond to one Hb atom and one Hc atom in the ethyl ester, or Hc and Hd in the allyl ester (when using a catalyst that generates *cis*-only product).

Figure 2: Comparison of heteronuclear J_{HC} couplings derived from DFT simulations (6-311++(d,p) basis set) and NMR experiments. a): Correlation between simulated and experimentally-measured ${}^nJ_{\text{HC}}$ ($n > 1$) in all samples. A linear fit to the data is shown, along with the corresponding Spearman's rho and P value of statistical significance. b): Bland-Altman analysis of the mean and difference in absolute J_{HC} values calculated from the two methods. The mean difference and ± 2 standard deviations from the mean are shown by solid and dashed lines, respectively.

Figure 3: Example HMBC data acquired from samples of $[1-^{13}\text{C}]$ -labeled vinyl acetate (top) and ethyl acetate (bottom).

Figure 4: CLIP-HSQMBC data acquired from $[1-^{13}\text{C}]$ -labeled propargyl pyruvate, using a selective excitation of Ha protons. The inset shows an expanded view of the projection of the crosspeak at the frequency of the ^{13}C carbon.

Figure 5: sel-HSQMBC-TOCSY data acquired from $[1-^{13}\text{C}]$ -labeled propargyl pyruvate, using a selective excitation of Hb protons. α and β data, defined as per conventional IPAP analysis: $\alpha = \text{IP} + \text{AP}$; $\beta = \text{IP} - \text{AP}$, are shown overlaid. The inset shows the projection at the frequency of the ^{13}C carbon and Hc protons. J_{HC} is derived from the horizontal displacement of the α and β data.

Figure 6: Contour plots of simulated maximum ^{13}C polarization as a function of J coupling values in a 3-spin system (para- H_2 , ^{13}C ; HH_1C) for three cases: a) magnetic field cycling (at a fixed adiabatic remagnetization time of 5 sec), b) PH-INEPT+, and c)

ESOTHERIC spin order transfer methods.

Figure 7: Illustration of the achievable ^{13}C polarization in allyl acetate by magnetic field cycling when considering only direct (through 4/5-bonds) polarization transfer (3-spin system) compared with when considering the complete neighboring heteronuclear and homonuclear J coupling network (6-spin system; “all spins”). The dash-dot lines show the effect of including estimates of the ^1H and ^{13}C relaxation, as discussed in the main text.

Table 1: Summary of experimentally-derived heteronuclear ${}^nJ_{\text{HC}}$ ($n > 1$) couplings in compounds investigated in this work.

${}^nJ_{\text{HC1}}$ (Hz)	Compound				
	VA	EA	EPR	AA	PP
${}^2J_{\text{HaC1}}$	-7.0°	-7.0°	-7.5^{\square}	-6.73^{\square}	–
${}^3J_{\text{HaC1}}$	–	–	–	–	1.35^{\square}
${}^3J_{\text{HbC1}}$	2.9°	3.1°	2.80^{\square}	3.15^{\triangle}	2.80^{\square}
${}^3J_{\text{HcC1}}$	–	–	2.08^{\square}	–	–
${}^4J_{\text{HcC1}}$	0.55^{\triangle}	-0.13^{\triangle}	–	-0.18^{\triangle}	–
${}^4J_{\text{HdC1}}$	-0.95^{\triangle}	–	-0.14^{\triangle}	–	–
${}^5J_{\text{HcC1}}$	–	–	–	–	0.27^{\triangle}
${}^5J_{\text{HdC1}}$	–	–	–	0.20^{\triangle}	–
${}^5J_{\text{HeC1}}$	–	–	–	0.08^{\triangle}	–

\circ : ${}^{13}\text{C}$ spectroscopy

\square : CLIP-HSQMBC

\triangle : sel-HSQMBC-TOCSY

Figure 1
[Click here to download high resolution image](#)

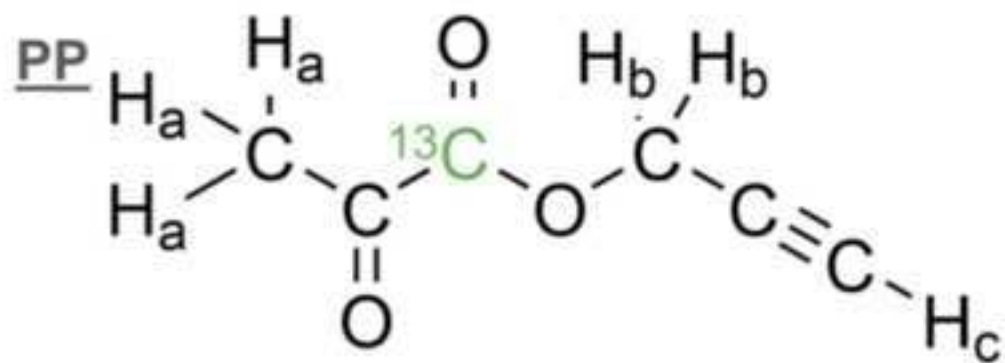
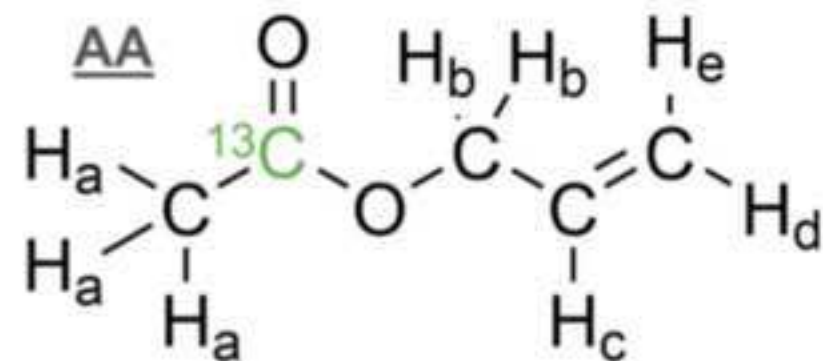
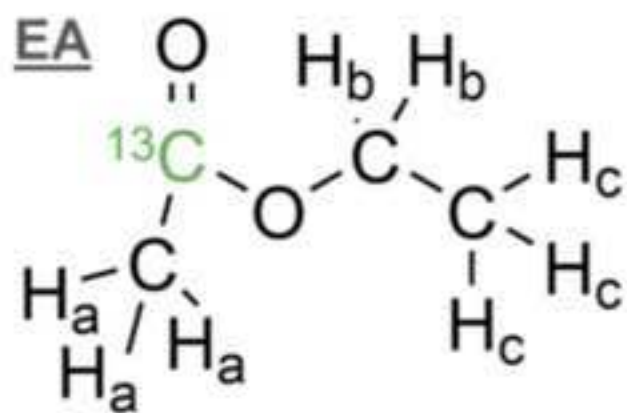
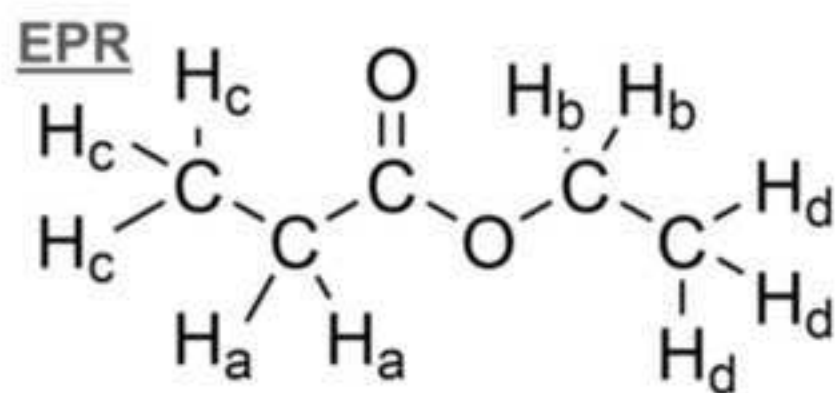
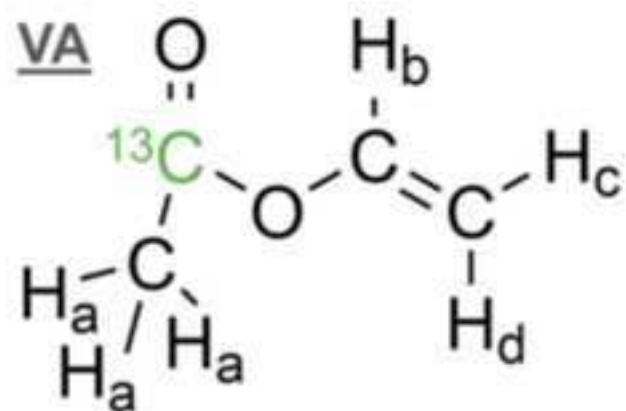


Figure 2
[Click here to download high resolution image](#)

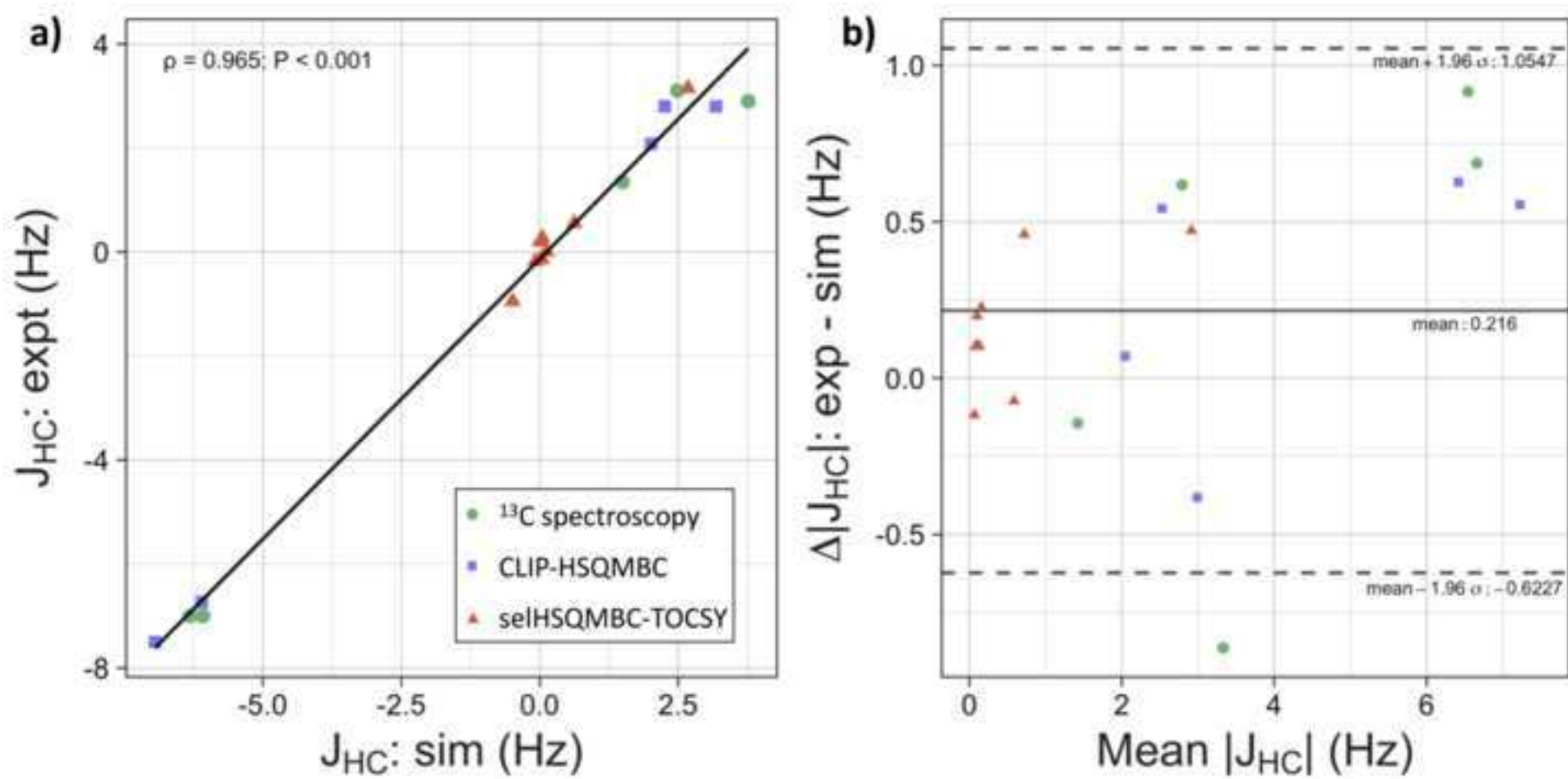


Figure 3
[Click here to download high resolution image](#)

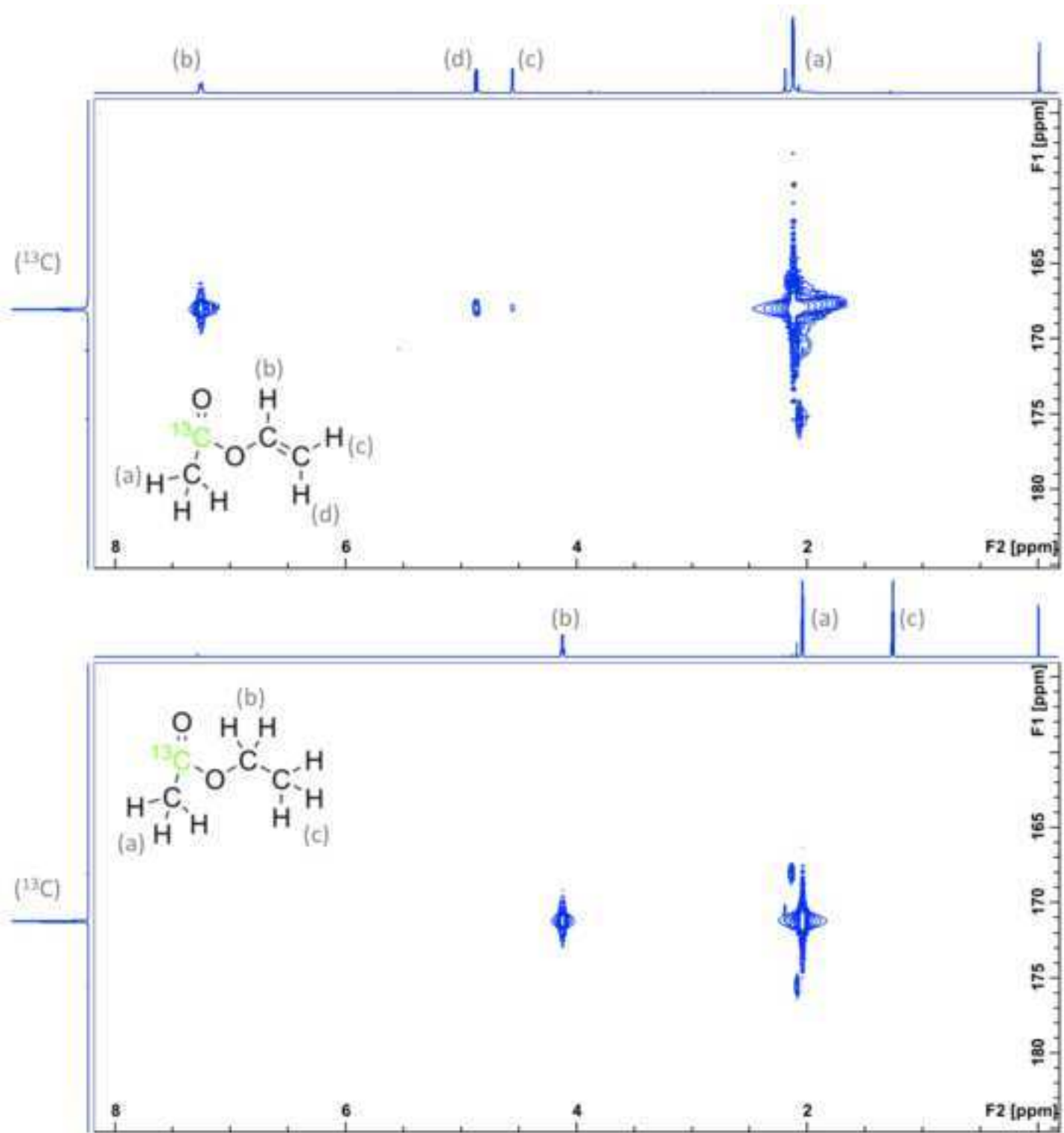


Figure 4
[Click here to download high resolution image](#)

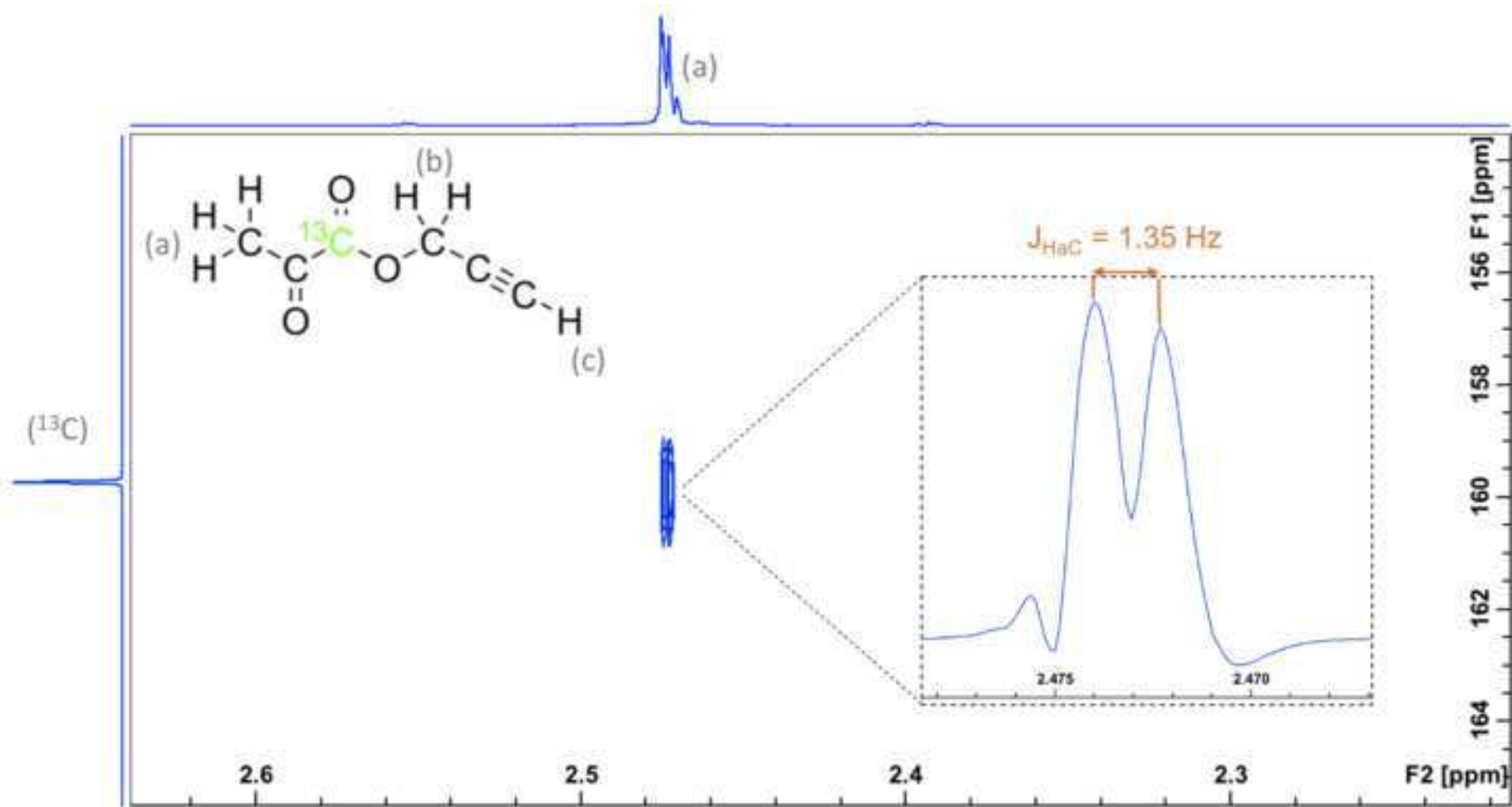


Figure 5
[Click here to download high resolution image](#)

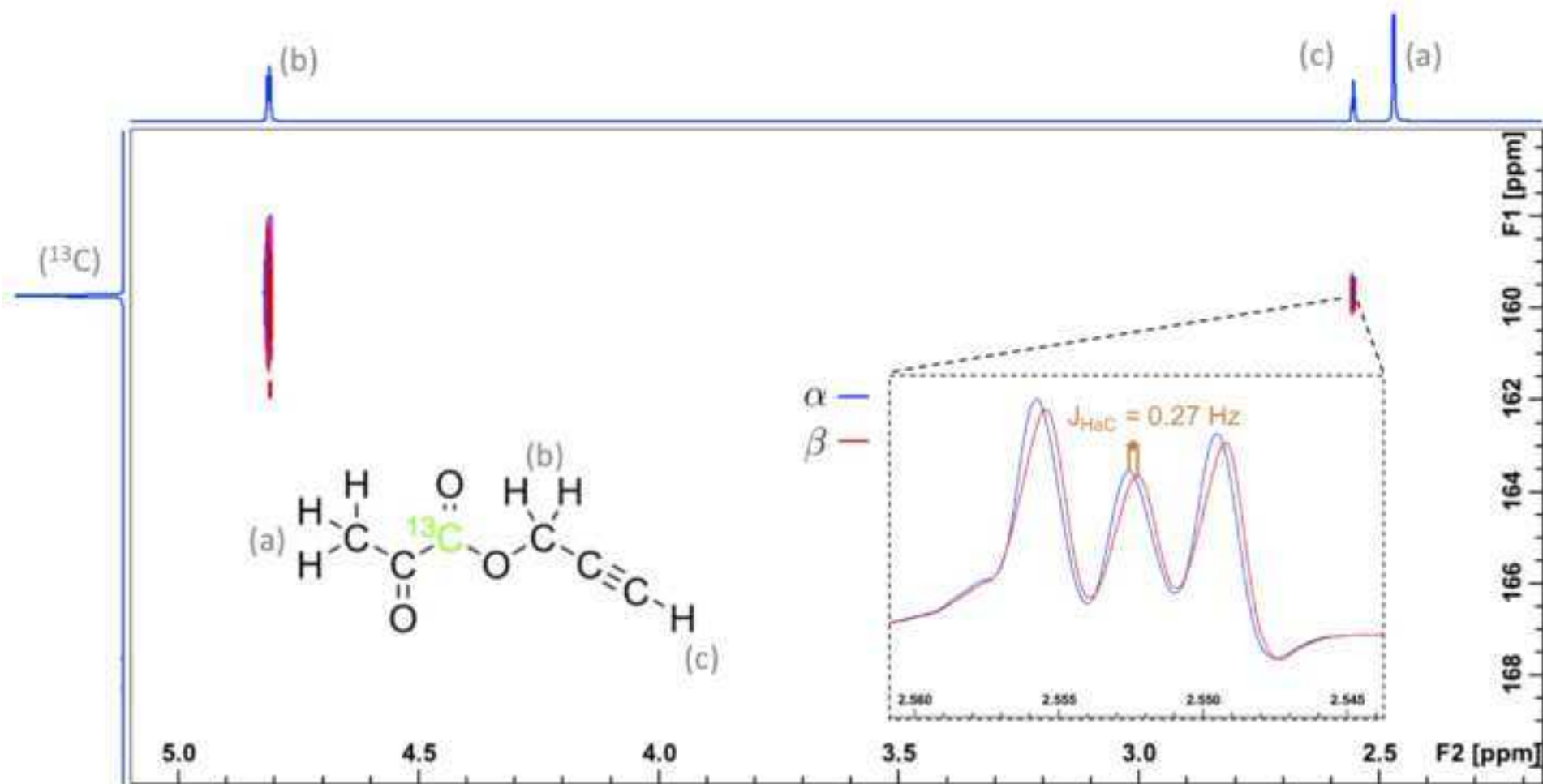


Figure 6
[Click here to download high resolution image](#)

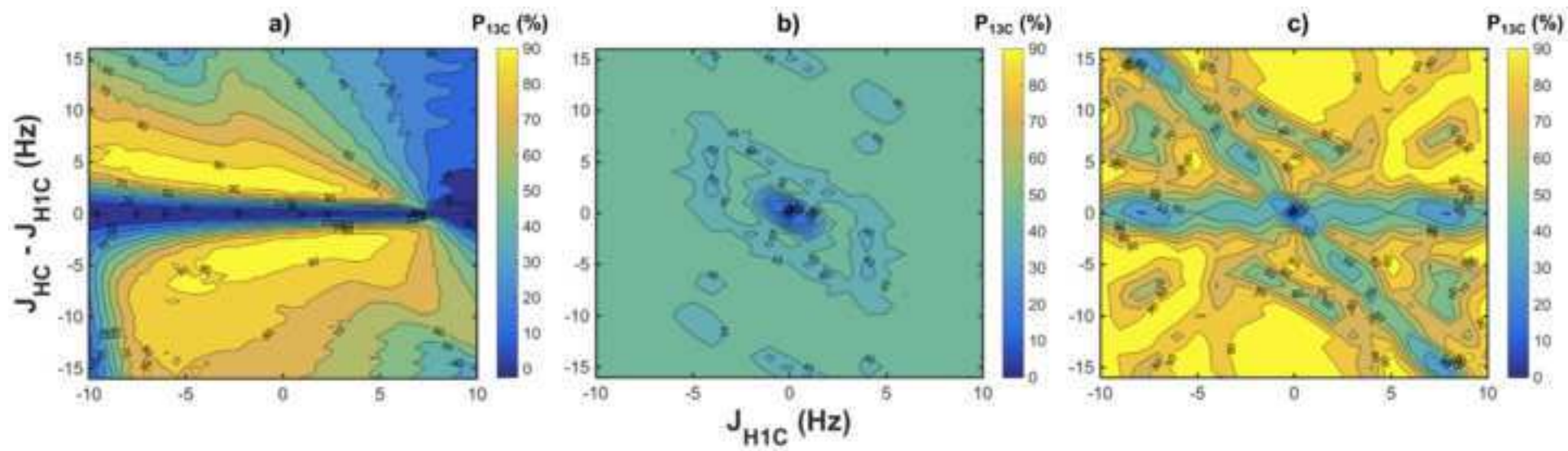


Figure 7
[Click here to download high resolution image](#)

